N87-29863

GRABBER ARM MECHANISM FOR THE ITALIAN RESEARCH INTERIM STAGE (IRIS)

Edmondo Turci*

ABSTRACT

Two deployable arms, named "grabbers," were designed and manufactured to provide lateral stability of the perigee spinning stage which will be deployed from the Space Shuttle cargo bay. The spinning stage is supported by a spin table on a cradle at its base. The Italian Research Interim Stage (IRIS), which is being developed under an Italian "Consiglio Nazionale delle Ricerche/Piano Spaziale Nazionale" (CNR/PSN) contract, is designed to carry satellites of intermediate mass up to 900 kg. The requirements are defined and the mechanism is described. Functional test results are presented.

INTRODUCTION

A grabber arm mechanism was designed to latch, at the upper level, the perigee spinning stage in the Space Shuttle cargo bay. This constraint will be remotely disengaged before the spinning and deployment of the stage. The mechanism consists of a set of rotating arms which enables a pin to engage and disengage with a mating socket. The withdrawal of the arm must give enough clearance to allow safe deployment of the stage. The technique is well known: a rotating plate enables a pin to engage in a socket, using a connecting rod and a motorized crank lever. This set of links provides a good lateral stiffness, as required, when the pin is forced into the socket. However, if there is a misalignment of the pin and the socket, then a high force is needed to lock the mechanism in position. This will cause high insertion forces on the interface structure with a consequent increase in mass.

GRABBER ARM MECHANISM

In order to achieve better locking performance and to save mass, a toggle action has been introduced into the linkage. (See fig. 1.) The grabber arm is driven upwards by a crank lever until it comes to rest against the interface structure. The crank continues to rotate forcing the toggle arms to expand. The toggle arms in turn move the sleeve upwards forcing out three swinging latches (pawls), which centralize the grabber pin in the socket. The mechanism then goes overcenter, locking the pin in position. The toggle arms are kept in position by springs (bottom washers) until the locking phase. The gap between the socket and the pin is large enough to allow for any relative displacement which could occur in the space environment. The pawls will still force the pin into the central position and the locking action of the toggle will provide a stiff connection.

*Aeritalia Space System Division, Turin, Italy.

Because of possible tangential misalignment after rotation of the spin table (i.e., in case of an aborted mission, the grabber must reengage the perigee stage before return of the Space Shuttle), a significant insertion force could occur. The grabber pin has a conical shape and is dry-lubricated to minimize this force.

The crank lever is driven by a geared stepper motor. Two sets of microswitches monitor the position of the crank lever.

Adjustment of the grabber pin is provided by rotating the two conical components; this eliminates misalignment due to manufacturing tolerances.

MECHANICAL INTERFACES AND LOADS

Cradle/Perigee-Stage Interface Characteristics

As already mentioned, after the grabber is inserted, the pin diameter is increased by the expansion of the pawls until the socket diameter is reached. During this phase, there is the capability to overcome (by means of the torque motor) any radial offset, up to a maximum of 1.5 mm, due to the space environment.

This capability is achieved by exploiting the cradle and tower (spinning stage and spin table) flexibility. The "y" direction stiffness is obtained from the IRIS mathematical model. Two different conditions are evaluated (fig. 2):

- With no grabber inserted, the system stiffness is minimum and is equal to 1620 N/mm.

- With one grabber inserted, the system stiffness is maximum and is equal to 5290 N/mm.

These values have been used for the calculation of the required motor torque characteristics assuming, as demonstrated by means of the NASTRAN model, that the stiffness along the x direction is lower.

Payload-Attachment-Fitting/Grabber Interface Characteristics

The payload attachment fitting (PAF) consists of an annular plate containing both bushings (sockets), which must offer a high resistance to the acting load. For this purpose, a hard Custom 455 alloy has been used. The grabber stiffness along the x and y directions can be considered approximately equal since the bearing and the plate are very stiff. It can be assumed that the grabber stiffness depends mainly on the deflection stiffness of the pawls.

Grabber/Cradle Interface Characteristics

To interface the grabber and the cradle, two fork brackets have been used. Each bracket has been joined to the cradle structure via four "HI-LOKS," which give a precise connection in both clearance gap and preload.

This connection is not removable and transmits high loads without depending on friction.

The motor is joined to the cradle by means of an attach fitting structure (fig. 3).

The stiffness of the crank lever attachment point, with the motor assembled to the cradle, has been calculated relative to the hinge pin. The minimum required stiffness is low and is easily satisfied by the motor attach fitting and cradle structure.

Flight Loads

The ultimate loads exchanged by the cradle and the PAF through the grabber are, in case of landing, a compression force of 95 000 N (on one grabber) and a tangential force of 58 000 N for both landing and lift-off cases. These loads are derived from the IRIS system coupled-analysis finite-element model. A thermal analysis at system level and local analysis complete the inputs for the grabber design.

KINEMATIC ANALYSIS OF THE GRABBER ARM

The kinematic ralationships of the linkage and the functional relationships of the forces acting on each part of the grabber have been investigated.

A fundamental hypothesis used is that concerning the tribological properties. A generalized friction cofficient has been used (molybdenum disulfide (MoS_2) - bonded solid lubricant in vacuum) for all the contact surfaces. Manufacturer's data sheet (and MIL-L-25504) shows values of friction coefficient of 0.05 for Hertz pressures comparable to those foreseen on the main critical parts. In order to comply with a more realistic distribution of pressures and other uncertainties, a value of f = 0.15 has been considered.

The model to be used for the linkage depends on the particular position reached by the articulated quadrilateral.

- Deployment: The gear motor rate is constant and the grabber head is driven toward the socket (on the PAF) up to the first contact. The required torque must only overcome the friction on the bearing due to the preload force and the grabber weight (ground tests).

- Spin-table misalignment recovery: The insertion of the grabber head into the socket initiates the misalignment recovery. The gear motor rate is still constant but additional torque is required because of the misalignment of the spin table with respect to the grabber position. The force along the insertion axis must not open the pawls until full insertion has been reached. The upper

spring washer and pawls are designed to ensure this condition.

- Pawls expansion and locking: The head of the grabber has been fully introduced in the socket. From this moment, any further rotation of the crank lever overcomes the elastic reaction of the upper spring washers forcing the internal sleeve upwards to open the pawls. As soon as the pawl is in contact with the socket, further expansion requires the crank lever to overcome the "system stiffness." That is, the complete IRIS spinning stage is forced to move by the expansion of the pawls.

The main points investigated were as follows.

Toggle Action

The toggle arms operate as a device which assures the mechanical lock of the grabber head into its proper hole. The model is sketched in fig. 4a. The locking is due to the overcenter position reached. This overcenter has a permanent equilibrium position, which is kept by the connection rod.

Expandable Head

The expandable head contains the locking and unlocking parts of the grabber. This occurs when the grabber plate is stopped and the internal levers are in movement. The model used is sketched in fig. 4b/c. The locking action can be considered as three successive phases:

- The pawl expansion begins and both upper and bottom spring washers are deflected until the gap is zeroed.

- The radial offset between socket and pin begins to be overcome. In the counteract worst condition, only one pawl works and develops the necessary force to the system stiffness.

- The radial offset has been completely recovered and the final position of the toggle arms has been reached. All three pawls are in contact within the socket. The bottom spring washer ensures that an adequate pressure is applied by each pawl on the socket internal surface. If the radial offset is zero, the pressure forces on each pawl are symmetrical and do not depend on the system stiffness. The grabber is then fully locked.

Free Expansion of the Pawls

This analysis evaluated the optimum profile of the pawls and the sleeve, and the axial contact forces. Because of the complexity of the profiles, a numerical computation was carried out.

The axial force on the sleeve and the pawl deflection vs. sleeve displacement in the free condition are represented in the diagram of fig. 4c.

Drive Torque

Evaluation of the drive torque on the crank lever from the withdrawn position to full locked position is a primary task of the analysis. The drive torque "C_M" will vary with the crank lever angle "ϕ" as shown in fig. 5. The phases considered were:

- Deployment
- Misalignment recovery (insertion)
- Locking
- Unlocking

The assumptions were:

- The deployment considers a constant drive motor angular rate, gravity, and friction torque on the grabber bearings. Inertia is neglected.
- The misalignment recovery assumes a spin-table friction torque of 50 N-m and a misalignment error of 15 mm (equivalent to a degree of rotation).
- The locking phase considers a radial offset (max 1.5 mm) and a nominal system stiffness (6600 N/mm) with one grabber inserted (worst case). The motor still maintains an unpowered torque to react flight loads (30 N-m).
- The locking/unlocking phase utilizes a generalized friction coefficient ($f = 0.15$).

MATERIAL USED IN THE GRABBER MECHANISM

The grabber plate was made from 7075 aluminum alloy. This choice is due to thermal displacement of the cradle interface fork brackets. The cylindrical tube, the cone, the eccentrics, and the crank lever are 15-5-PH steel. The pawls and the sleeve are Inconel 718 hardened with thick chromium coating. The socket is Carpenter Custom 455. The thermal properties of the materials are adequately matched. All sliding parts are dry-lubricated with resin-bonded solid-film molybdenum disulfide of the type available today for space applications. Functional tests were conducted early in the development to verify local conditions of the sliding parts at appropriate Hertz contact pressure and coefficients of friction. Chromium coatings were introduced during these preliminary tests. The rotating hinges of the grabber plate utilize space-qualified bushings.

REDUNDANCY PROVISIONS

Redundancy has been incorporated into the grabber design to prevent single-point failures from making the grabber inoperative. The motor has two isolated redundant windings and electronic control units. The design uses a brushless permanent-magnet stepper so that none of the problems associated with contacting electrical interfaces in vacuum can occur. The speed reducer uses the harmonic drive concept (Schaeffer Magnetics). The upper and lower spring washers can provide enough force even when a single spring has failed. Rotating parts are bushed and designed to last one order of magnitude times the required life. Three switch mechanisms have been used for any of the two extreme operating conditions (withdrawn, locked).

The structural elements which are not redundant will be investigated extensively during qualification and fracture analysis tests.

MOTOR AND INTERFACE CHARACTERISTICS

Each grabber has an actuator that is joined to the cradle structure by means of an attach fitting. This consists of two straps and a motor support at the junction to the cradle. (See fig. 3.) The actuator comprises the following major elements: (1) motor, (2) speed reducer, (3) output flange, (4) motor housing, (5) frame, and (6) bearings. The stepper motor uses samarium-cobalt magnets and is three-phase "y" connected, designed for six-state bipolar drive.

The drive scheme sequentially excites each of the three motor phases in a bipolar mode, thus producing the required six magnet states that result in stepwise motion of the motor. By reversing the order, direction of rotation is reversed. Maximum rate is 300 steps per second. The available torque on the shaft is normally 200 to 240 N-m and 110 N-m when a failure on the windings has been introduced. The motor has been fully space qualified by Schaeffer Magnetics under Aeritalia specification.

DEVELOPMENT TESTS

In June/July 1985, a grabber development prototype was tested. The test utilized a fixture simulating the cradle/spinning-stage interfaces, including spin-table movement. (See fig. 6.)

The stiffness of the structure was simulated by springs and appropriately dimensioned plates and rods. The crank shaft was rotated manually, the torque and crank angles being measured at each step.

The main scope of this test was to confirm the maximum torque needed and to verify the tribological improvements introduced on the development prototype. (Chromium coating on pawls and sleeve was not used in the preliminary tests.)

Five tests have been performed with differnent values of radial offset (ε_r) and spin-table misalignment recovery (ε_c). The test results are given in table I.

Significant findings were made when comparing the results of test no. 4 with the theoretical values as shown in fig. 5:

- The spin-table misalignment recovery required a drive torque of 25 N-m (crank angle 100/110 deg) from both calculated and measured methods.

- The maximum measured drive torque in locking operation was 52 N-m, whereas the calculated value was 89 N-m.

The following explanation is suggested. The assumed generalized value of the friction coefficient f = 0.15 is conservative where high contact pressures are applied; that is the case of the locking operation. The value f = 0.15 is correct when moderate contact pressures are applied; that is the case during the insertion for misalignment recovery.

As a resin bonded solid film MoS_2 has been used on sliding surfaces, a more realistic analysis should consider f = 0.05 where high contact pressures are applied and f = 0.15 where moderate pressures are applied.

When the grabber was disassembled, there was no evidence of crushing or coating removal.

QUALIFICATION TESTS

Thermal vacuum and fracture mechanics tests are programmed to be completed by the middle of 1987.

Thermal Vacuum Test

The qualification grabber model will be installed on a test fixture simulating the attachment point of the cradle structure and the PAF coupling section. The test fixture is similar to that used for the grabber development test modified to support the electric motor and suitable to be used in a thermal vacuum chamber.

The test article assembled on the test fixture will be placed in a test suspension allowing its fitting inside the vacuum chamber. Cryogenic shrouds and a set of infrared lamps will be inserted in order to obtain the

required cold and hot conditions during the test. Fig. 7 illustrates the thermal vacuum test setup showing both the grabbers and the test fixture.

The test article equipped with a set of strain gauges and thermocouples will be subjected to a set of complete functional cycles in nominal and misaligned positions. The thermal cycling profile will be repeated as many as 35 times including spring and motor failure simulations. Determining functional life in the thermal vacuum environment and establishing capability of the tribological processes are the objectives of the test.

Load and Fracture Mechanics Tests

The grabber will be loaded utilizing mechanical interfaces and jacks to reproduce lift-off and landing conditions. A standard fracture mechanics procedure will be applied to the model grabber. These tests will complete the qualification test program.

CONCLUSION

The design described in this paper proved to be a suitable method to provide stiff structural constraints. Very good locking performance was achieved leading to mass savings since low insertion forces on the interface structure were required.

The grabber has been designed to a high level of reliability over a broad spectrum of environments. State-of-the-art technologies and lubricants have been used throughout.

TABLE I.- DEVELOPMENT TEST RESULTS: TORQUE VS. CRANK ANGLE

a. Engagement

Test 1; ε_r - 0 mm, ε_c - 0 mm		Test 2; ε_r - 0.5 mm, ε_c - 15.5 mm		Test 3; ε_r - 1 mm, ε_c - 15.5 mm		Test 4; ε_r - 1.5 mm, ε_c - 15.5 mm		Test 5; ε_r - 1.8 mm, ε_c - 15.5 mm	
Angle, deg	Torque, N-m	Angle, deg	Torque, N-m	Angle, deg	Torque, N-m	Angle, deg	Torque, N-m	Angle, deg	Torque, N-m
-22	2.2	105	10	95	10	95	25	107	10
-5	2.4	115	12	107	25	103	25	115	31
10	3	123	15	115	13	111	10	123	39
25	3.6	130	12	123	13	119	13	130	49
40	4.6	140	32	132	34	123	34	138	70
55	8	150	15	138	30	130	49	Locked	0
70	9	160	0	150	0	138	52		
85	10	Locked	0	Locked	0	150	0		
95	10					Locked	0		
111	9								
119	11								
130	12								
140	41								
Locked	0								

b. Disengagement

Test 1		Test 2	
Angle, deg	Torque, N-m	Angle, deg	Torque, N-m
Un-locked	-4	Un-locked	-5
150	9	140	8
130	7	130	8
107	8	119	8
90	8	111	8
70	5.5	70	4
55	4.4	40	0
40	3.3		
25	2.4		
10	1.6		
-22	1		

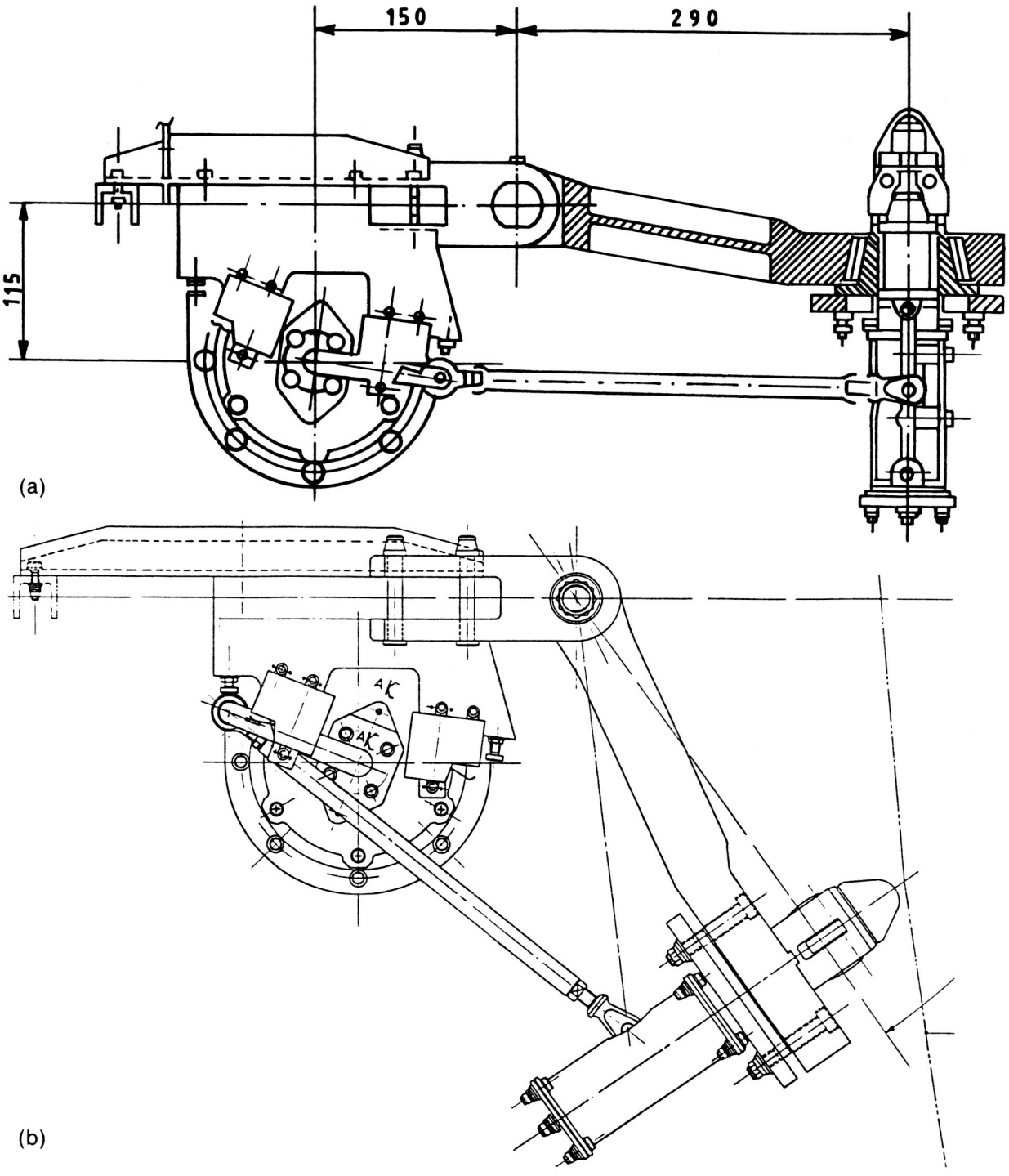

Figure 1. Grabber arm configuration (dimensions in millimeters). (a) Deployed. (b) Withdrawn.

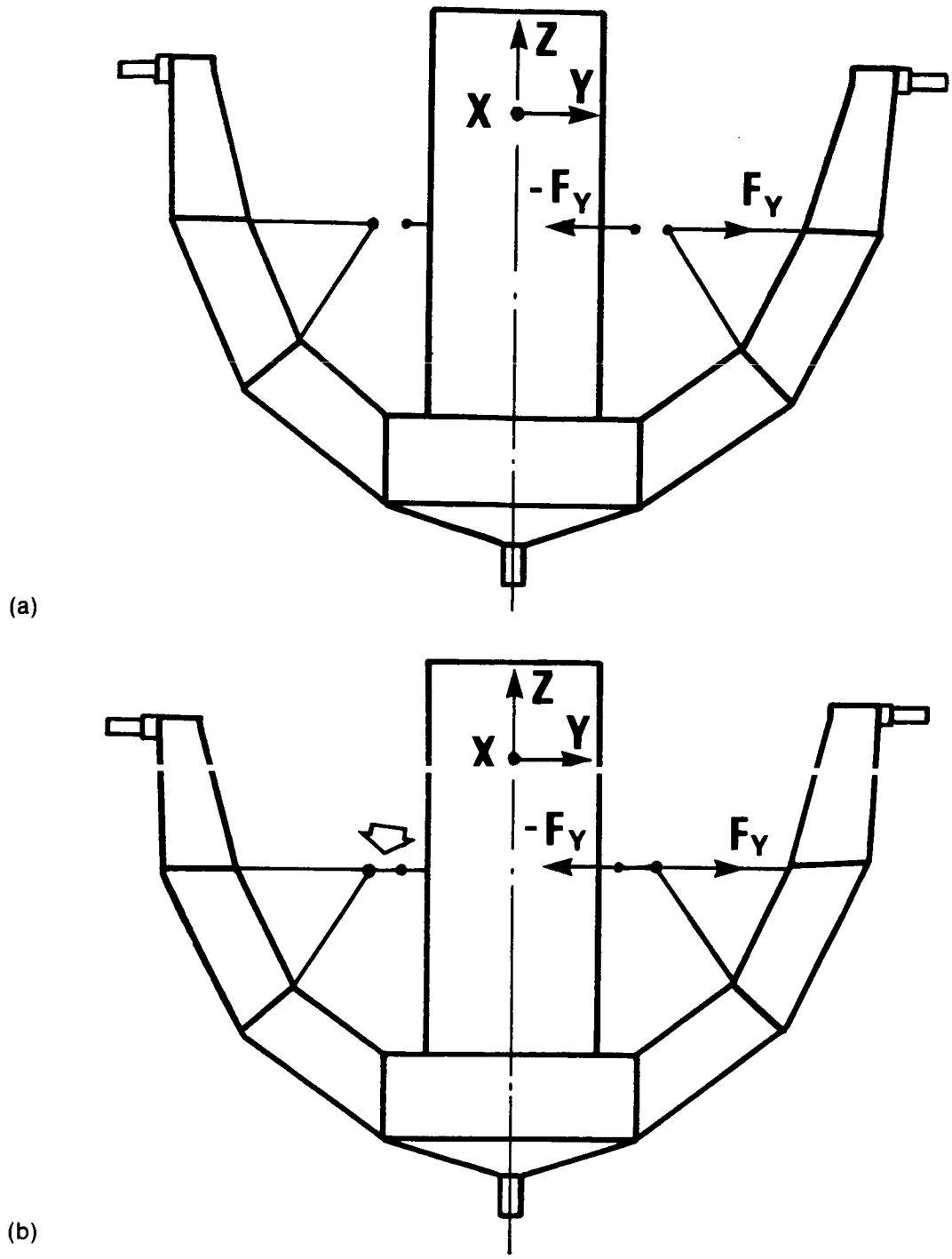

Figure 2. Cradle and spinning stage: grabber constraints. (a) Both grabbers open. (b) Both grabbers inserted.

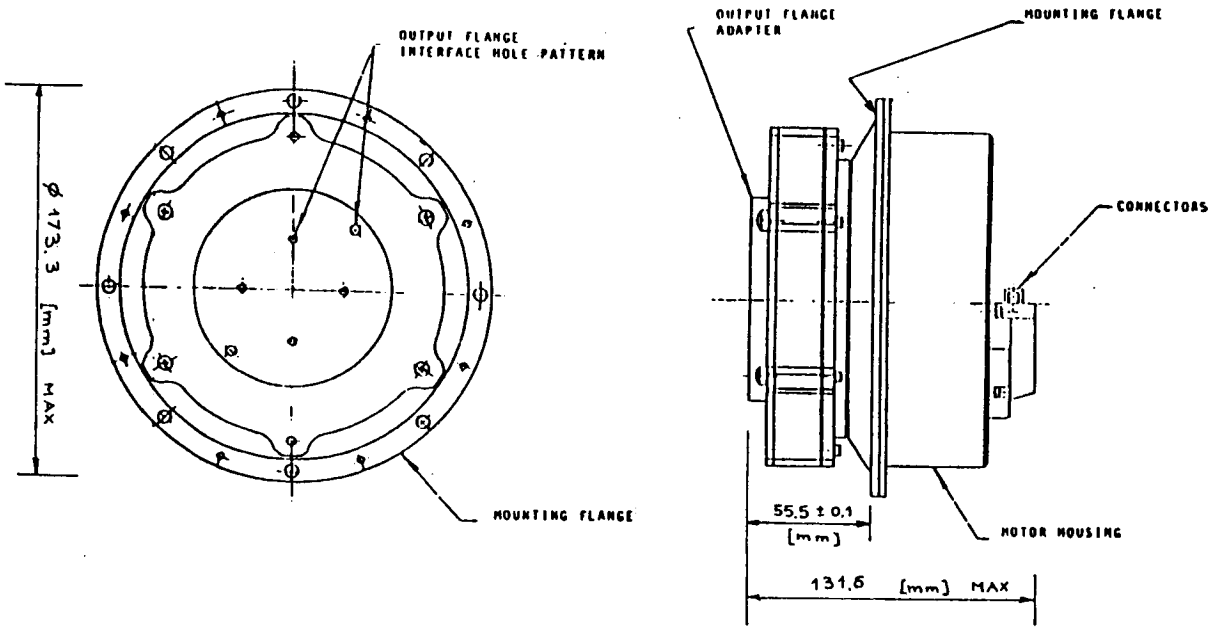

GRABBER ACTUATOR

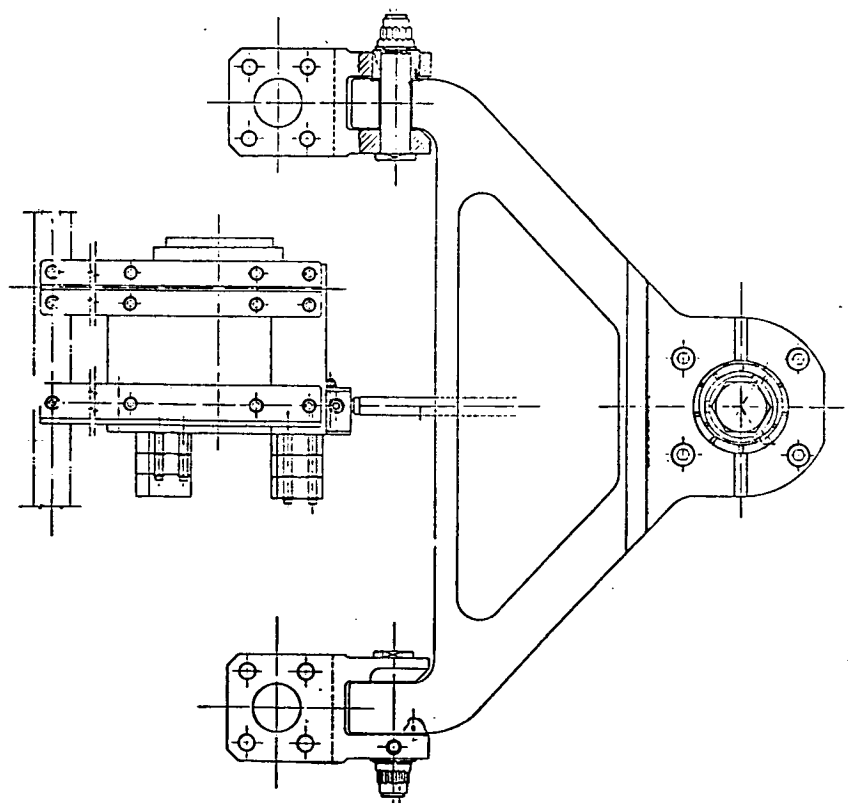

Figure 3. Grabber actuator and mechanical interfaces.

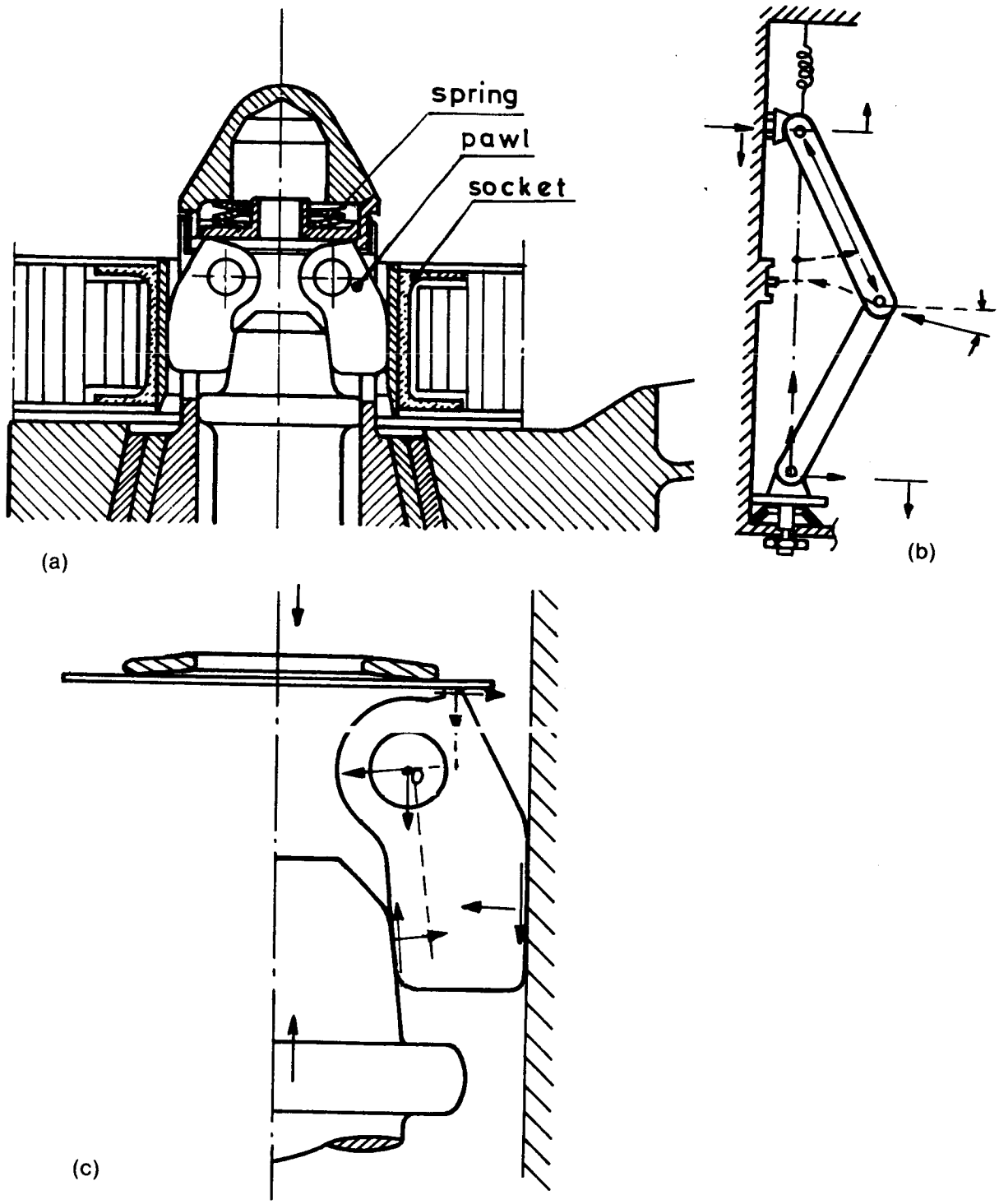

Figure 4. Linkages of the expandable grabber head. (a) Expandable grabber head. (b) Toggle arms. (c) Sleeve and pawls.

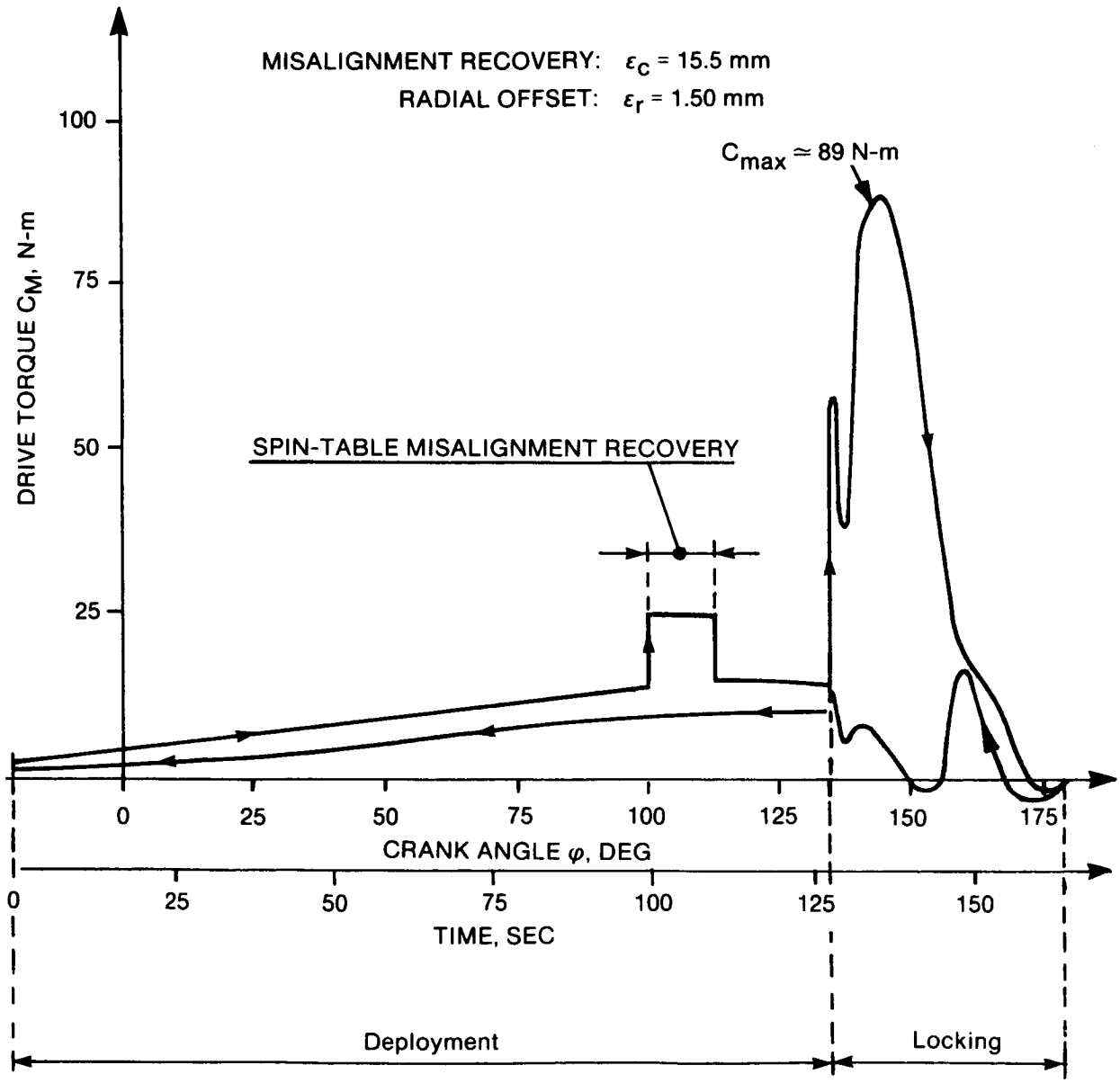

Figure 5. Drive torque versus crank rotation: diagram.

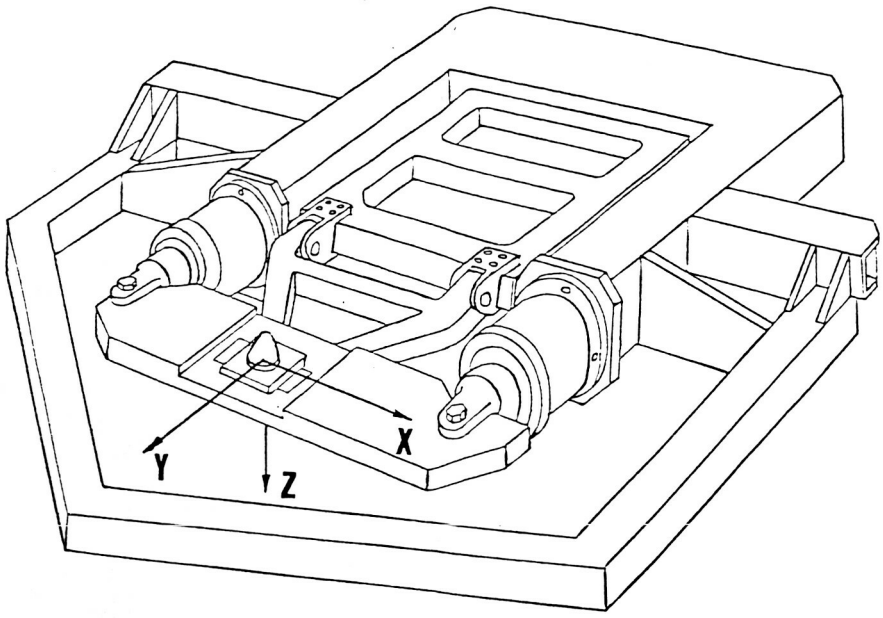

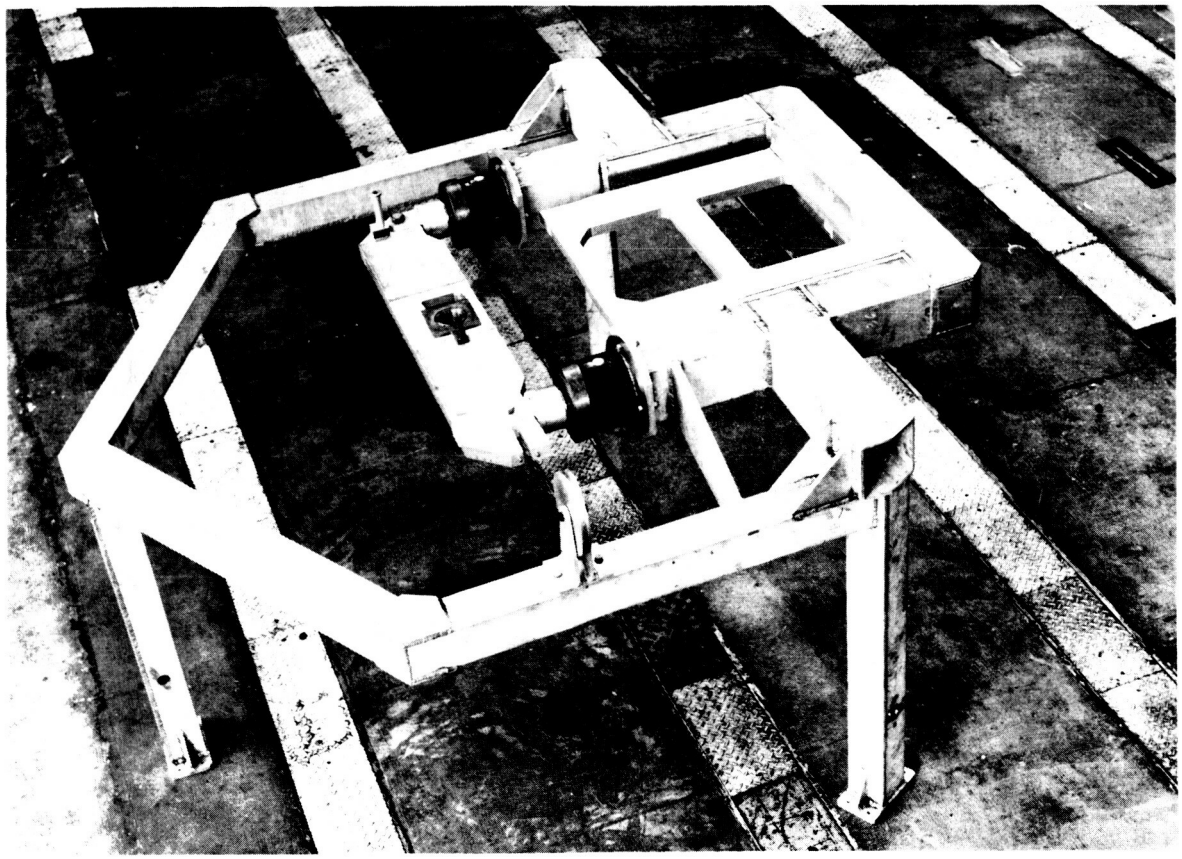

Figure 6. Test fixture simulating cradle/spinning-stage interfaces.

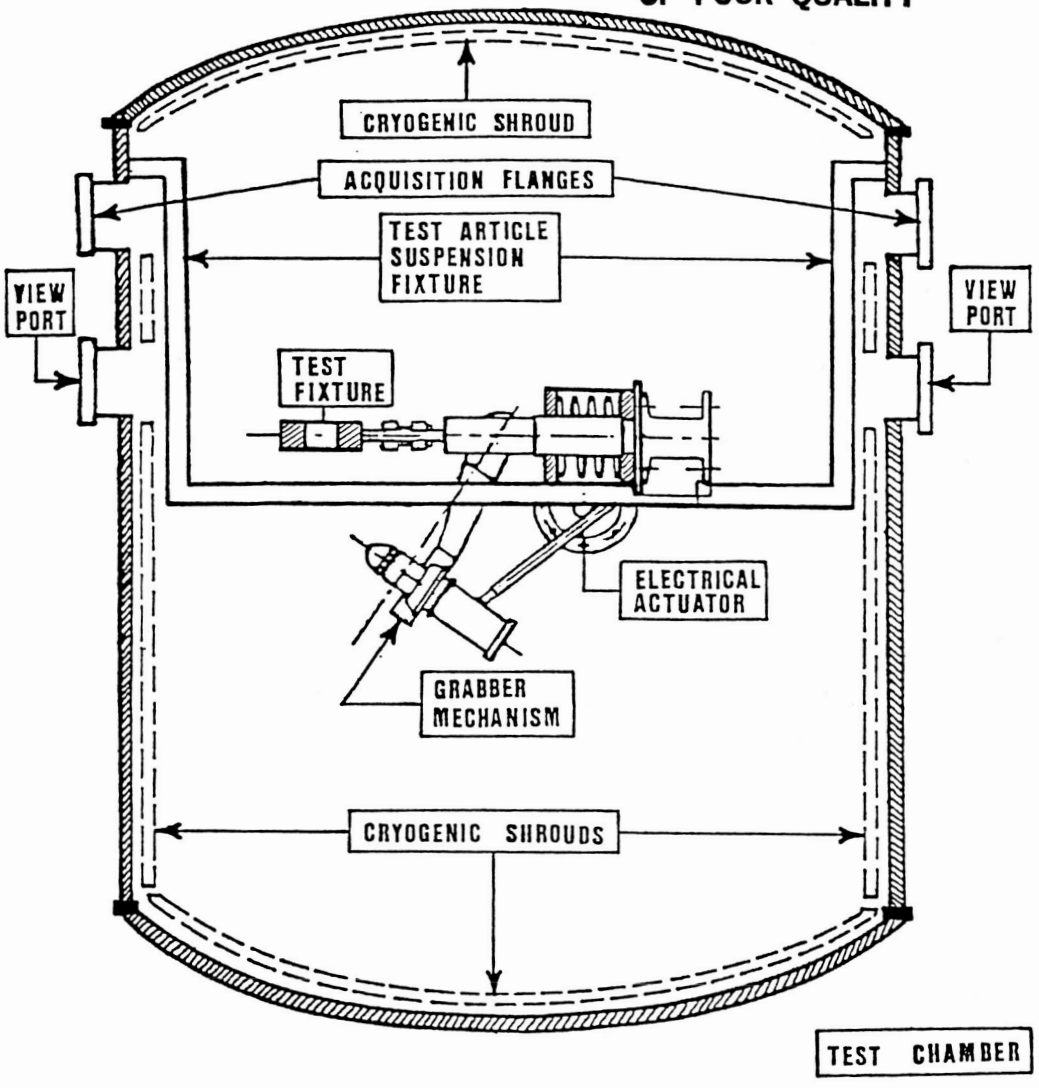

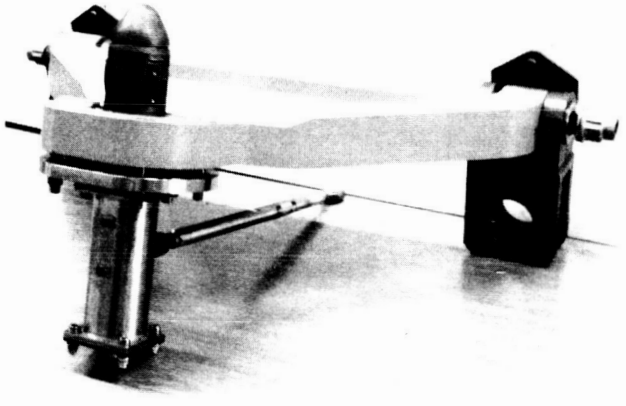

Figure 7. Thermal vacuum test setup and test item.